Comparison of Intergranular Degradations of Secondary NMC Particles in Liquid and Solid-State Batteries

Fernando D. Cúñez[1,4*], Radwa Elawadly[1], Eric Hintsala[2], Wonjoon Sun[3], Yiyang Li[3*], Qingsong Howard Tu[1*]

1) *Department of Mechanical Engineering, Rochester Institute of Technology, Rochester, 14623, NY, USA.

2) Bruker Nano Surfaces & Metrology, 9625 West 76th St, Eden Prairie, 55344, MN, USA.

3) Materials Science and Engineering, University of Michigan, Ann Arbor, 48109, MI, USA.

4) Department of Earth and Environmental Sciences, University of Rochester, Rochester, 14627, NY, USA.

*Corresponding author(s). E-mail(s): fcunezbe@ur.rochester.edu; yiyangli@umich.edu; howard.tu@rit.edu;

Support Information

I. Hiramatsu-Oka Model to estimate the fracture stress

The Hiramatsu–Oka model is an analytical solution used to interpret diametral compression ("crushing") tests of brittle spherical particles. In their derivation, the particle is idealized as an isotropic, linear-elastic sphere of radius R compressed between two platens by a uniform radial pressure applied over two small, opposite spherical caps (contact radius a). From the resulting stress field, one can estimate the maximum tensile (hoop/first principal) stress responsible for fracture and relate it to the measured failure load Fc as follows:

$$\sigma_T = \frac{\kappa F_c}{\pi R^2} \quad (1)$$

Where κ is a dimensionless proportionality factor that converts the nominal stress scale into the peak tensile stress predicted by the Hiramatsu–Oka stress solution at the onset of fracture. Physically, κ accounts for the non-uniform internal stress distribution created by the localized contacts (two caps) during diametral compression. It is not a fitted material property; it comes from the mechanics of the boundary-value problem. For the common experimental regime of small contacts (hard platens; small a/R), the Hiramatsu–Oka solution yields $\kappa \approx 0.7$(order unity), which is why many studies use a constant near 0.7 for brittle spheres under small-contact diametral compression.

II. DEM Model

In the DEM simulations, the contact force between two interacting bodies i and j is decomposed into a normal and a tangential contribution. For a contact with unit normal vector nij (pointing from particle j to particle i), the total contact force acting on particle i can be written as:

$$F_{ij} = (k_n \delta n_{ij} - \gamma_n v n_{ij}) + (k_t \delta t_{ij} - \gamma_t v t_{ij}) \quad (2)$$

Where: F_{ij} is total contact force exerted on particle i by particle j $[N]$. The contact force is decomposed into a normal and a tangential component. The normal component consists of an elastic spring term and a viscous damping term. Likewise, the tangential component includes an elastic shear term and a viscous damping term. The elastic shear term is history-dependent: it is computed from the accumulated tangential displacement (tangential "overlap") between the particles over the lifetime of the contact.

The variables in Eq. (2) are described as follows:

k_n is the elastic constant for normal contact, δn_{ij} is the overlap distance of 2 particles, γ_n is the viscoelastic damping constant for normal contact, vn is the normal component of the relative velocity of the 2 particles, k_t is the elastic constant for tangential contact, δt_{ij} is the tangential displacement vector between 2 spherical particles which is truncated to satisfy a frictional yield criterion, γ_t is the viscoelastic damping constant for tangential contact, and vt is tangential component of the relative velocity of the 2 particles.

The coefficients k_n, γ_n, k_t, γ_t are estimated from the material properties and the Hertzian model as follows:

$$k_n = \frac{4}{3} Y^* \sqrt{R^* \delta_n},$$

$$\gamma_n = -2\sqrt{\frac{5}{6}}\, \beta \sqrt{S_n m^*} \ge 0,$$

$$k_t = 8G^* \sqrt{R^* \delta_n},$$

$$\gamma_t = -2\sqrt{\frac{5}{6}}\, \beta \sqrt{S_t m^*} \ge 0.$$

$$S_n = 2Y^* \sqrt{R^* \delta_n}, \qquad S_t = 8G^* \sqrt{R^* \delta_n}$$

$$\beta = \frac{ln(e)}{\sqrt{ln^2(e) + \pi^2}},$$

$$\frac{1}{Y^*} = \frac{\left(1-\nu_1^{\,2}\right)}{Y_1} + \frac{\left(1-\nu_2^{\,2}\right)}{Y_2},$$

$$\frac{1}{G^*} = \frac{2(2-\nu_1)(1+\nu_1)}{Y_1} + \frac{2(2-\nu_2)(1+\nu_2)}{Y_2}$$

$$\frac{1}{R^*} = \frac{1}{R_1} + \frac{1}{R_2}, \quad \frac{1}{m^*} = \frac{1}{m_1} + \frac{1}{m_2}$$

Y...Young's modulus G...Shear modulus

ν...Poisson ratio e...coeff.of restitution

III. <u>Single Particle Electrochemical data, Scanning Electron Microscope (SEM) images, and Load vs Displacement curves for the 3 tested conditions for NMC532</u>

- 1 charge cycle

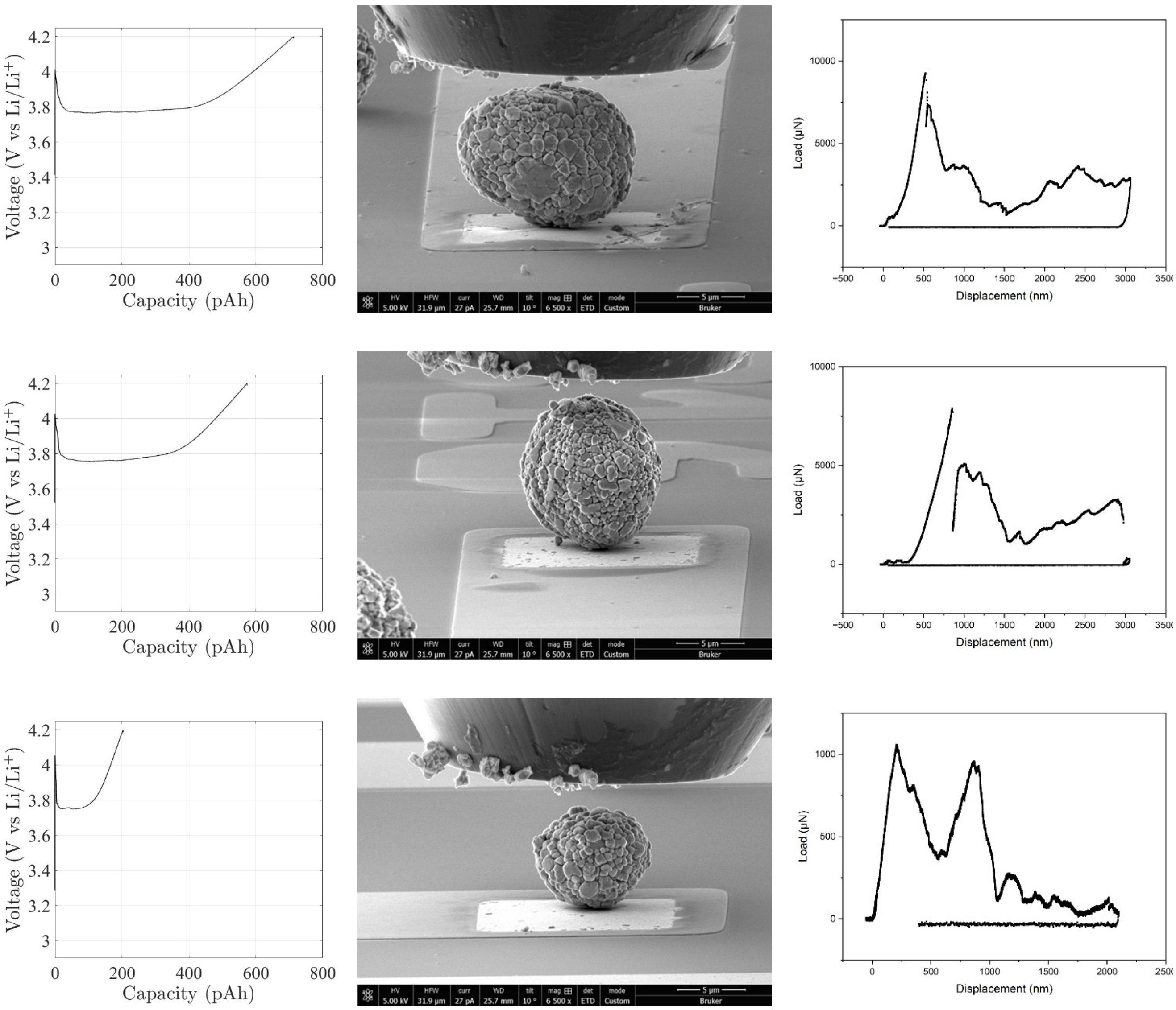

- 1 charge and discharge cycle

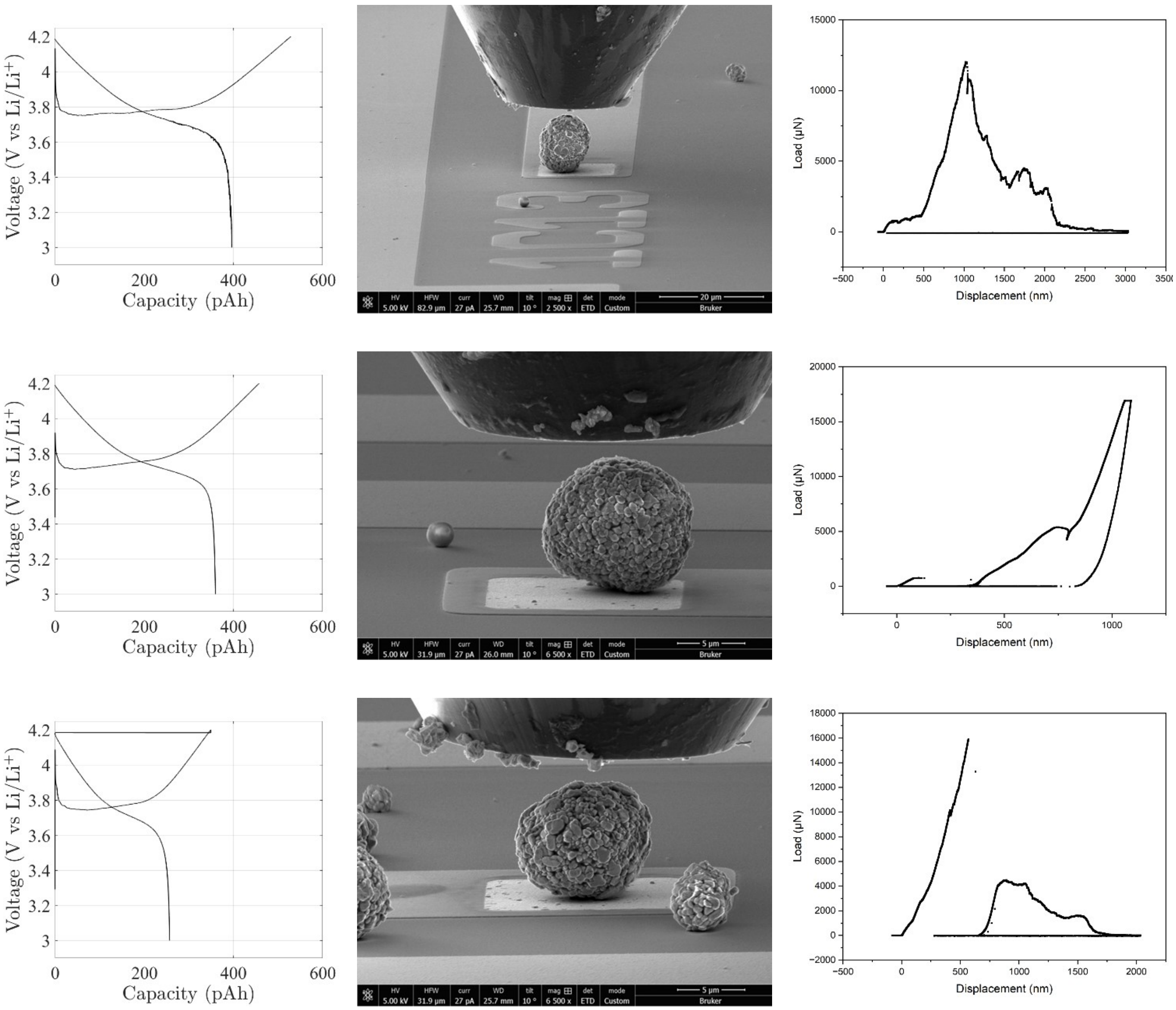

- 10 charge/discharge cycles

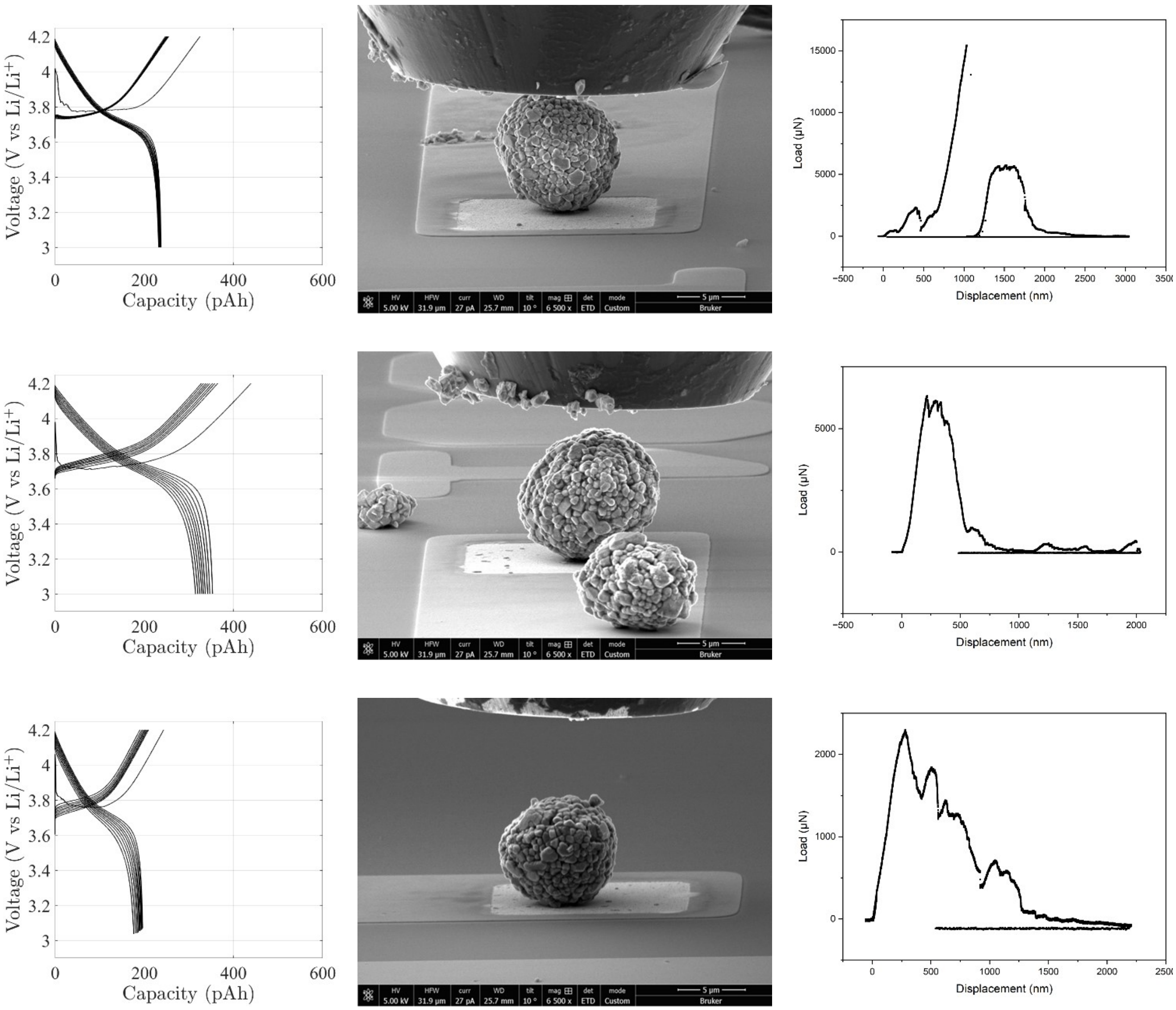
Voltage (V vs Li/Li+)
Capacity (pAh)
0
200
400
600
3
3.2
3.4
3.6
3.8
4
4.2
Load (µN)
Displacement (nm)
5 µm
Bruker

IV. <u>Single Particle Electrochemical data, Scanning Electron Microscope (SEM) images, and Load vs Displacement curves for the 3 tested conditions for NMC811</u>

- 1 charge cycle

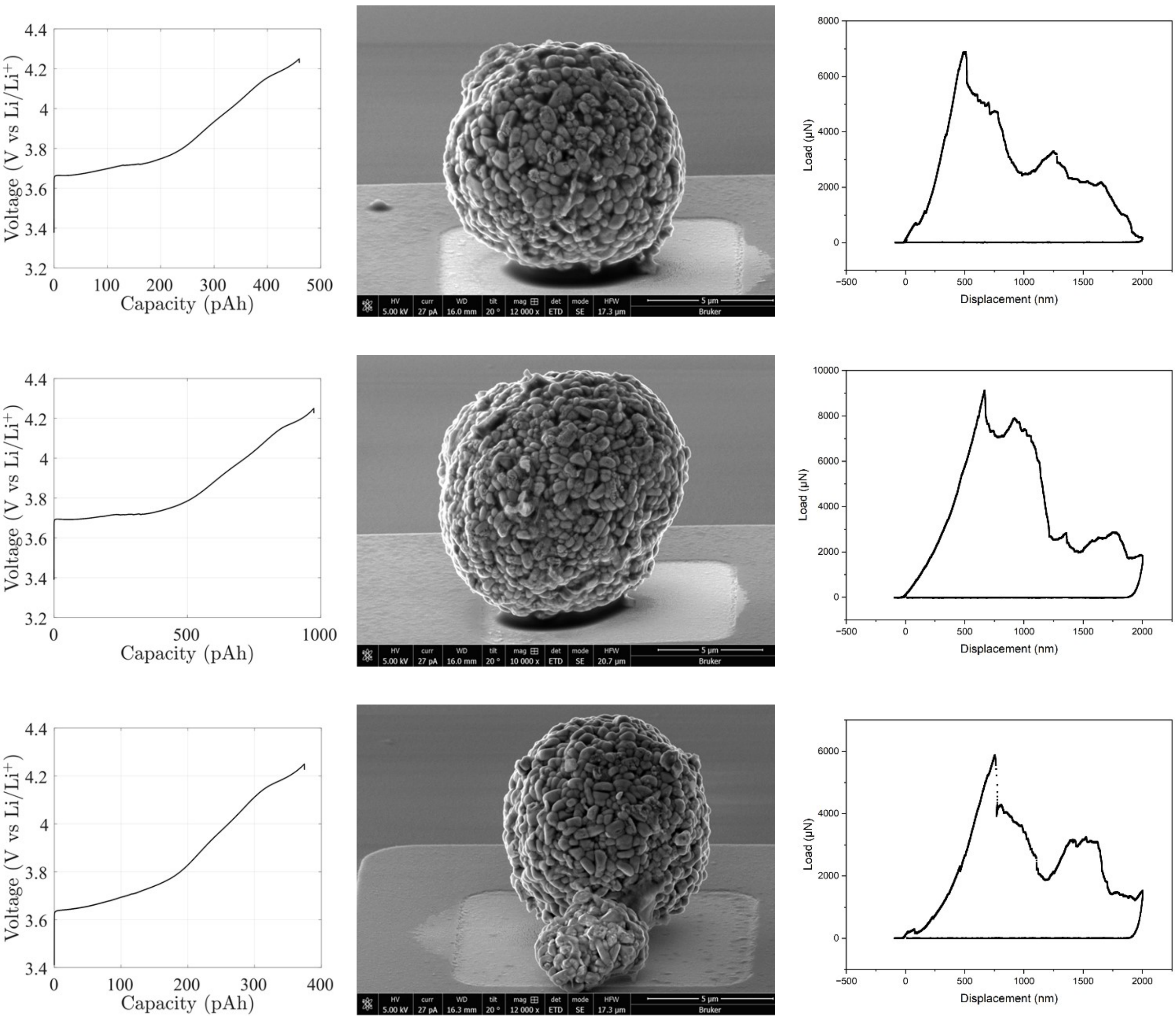

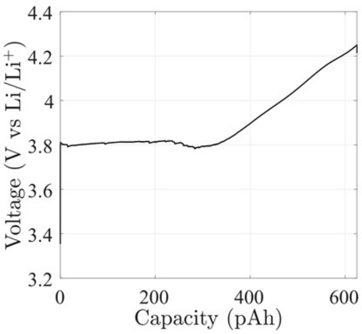

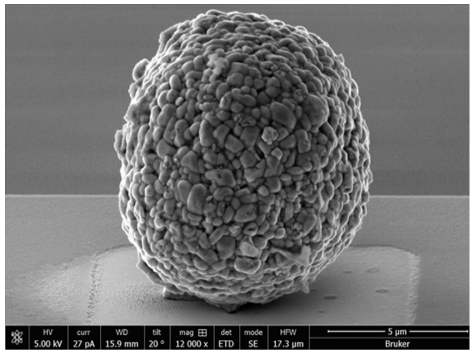

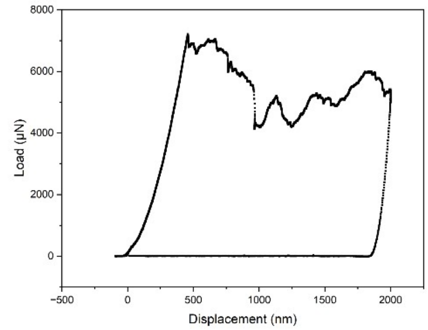

- 1 charge and discharge cycle

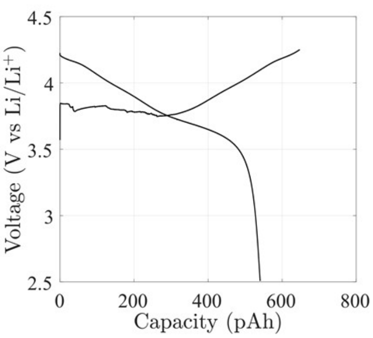

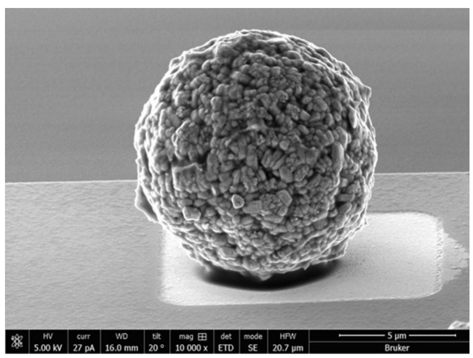

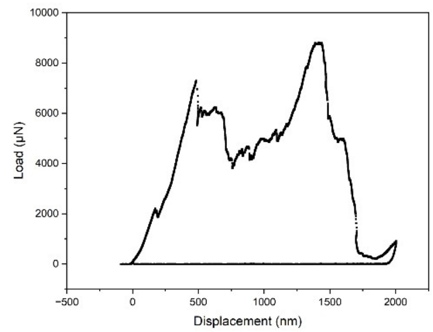

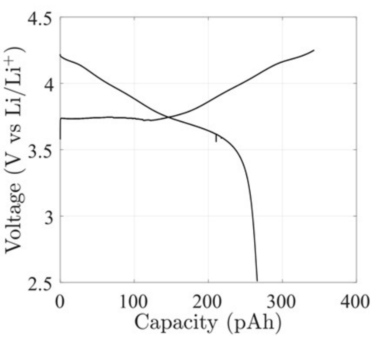

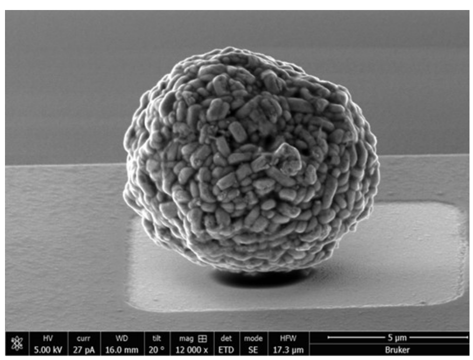

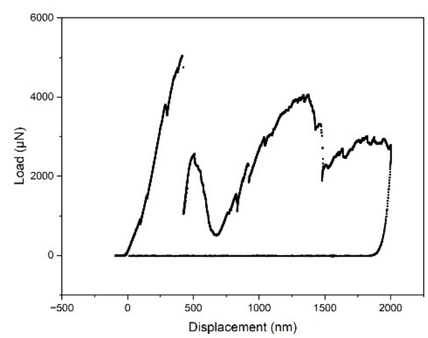

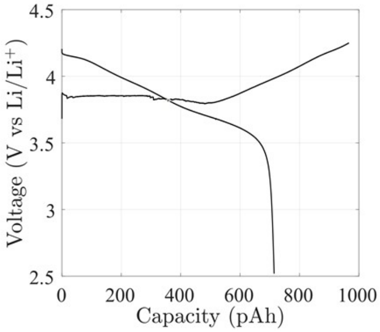

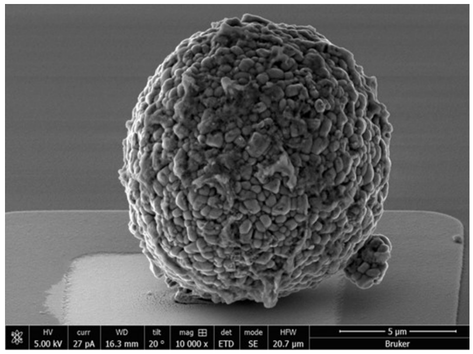

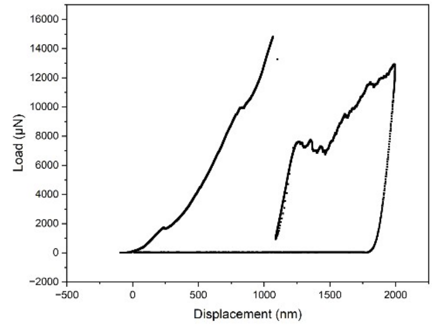

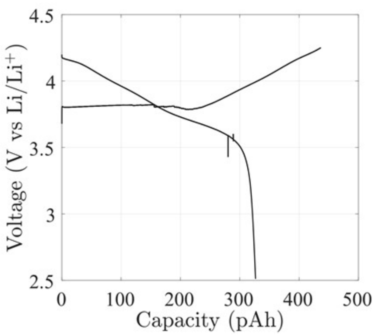

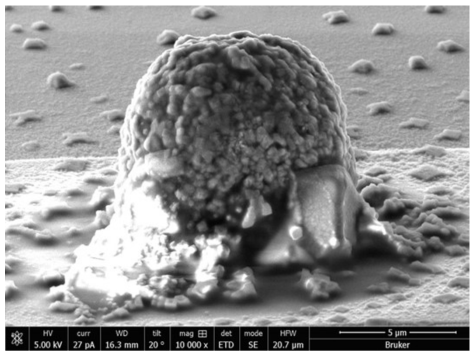

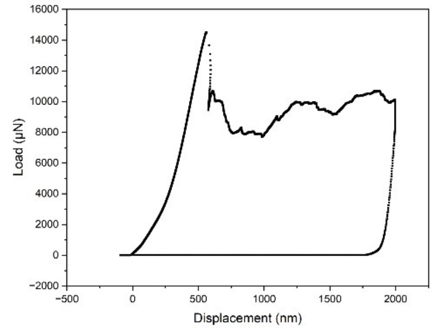

- 10 charge/discharge cycles

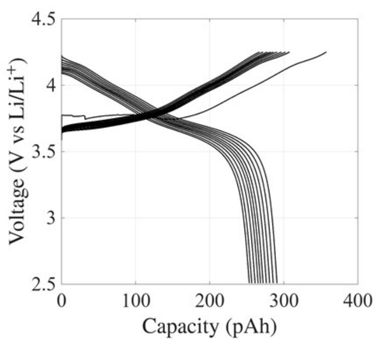

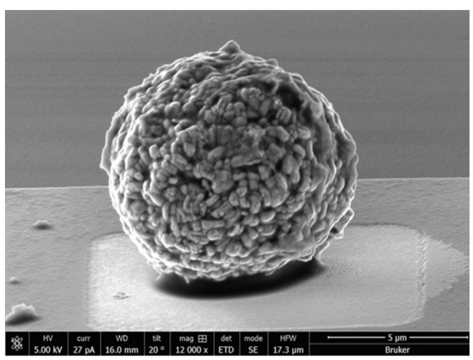

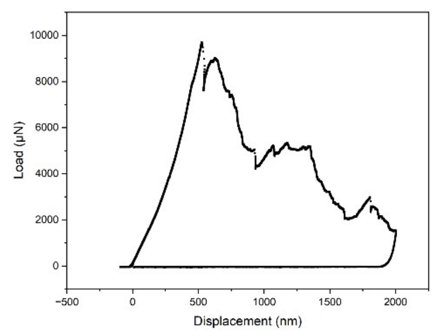

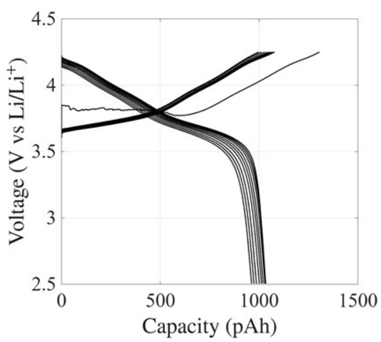

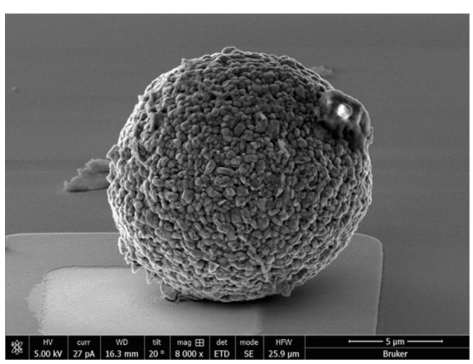

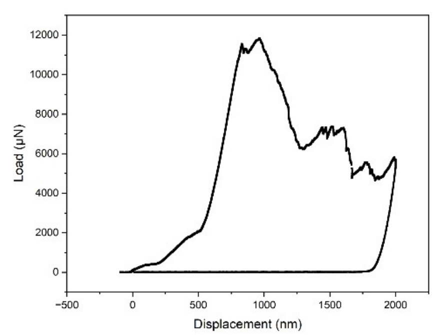

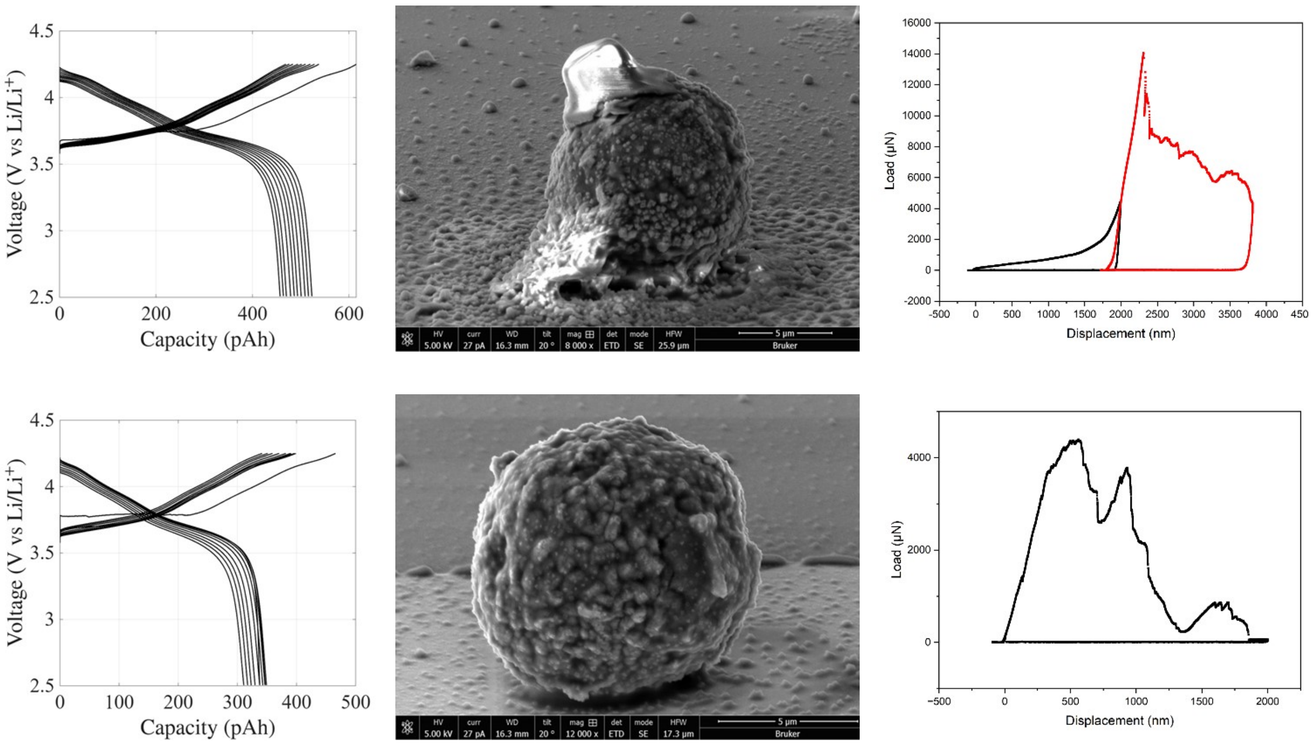

V. <u>Electrochemical data over 100 cycles in a all-solid-state battery fabricated under 300 MPa</u>

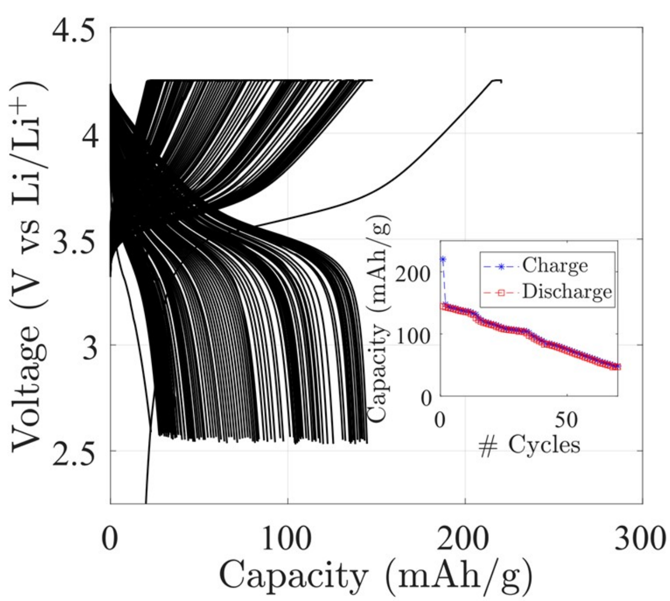

VI. Electrochemical data over 100 cycles in a all-solid-state battery fabricated under 500 MPa

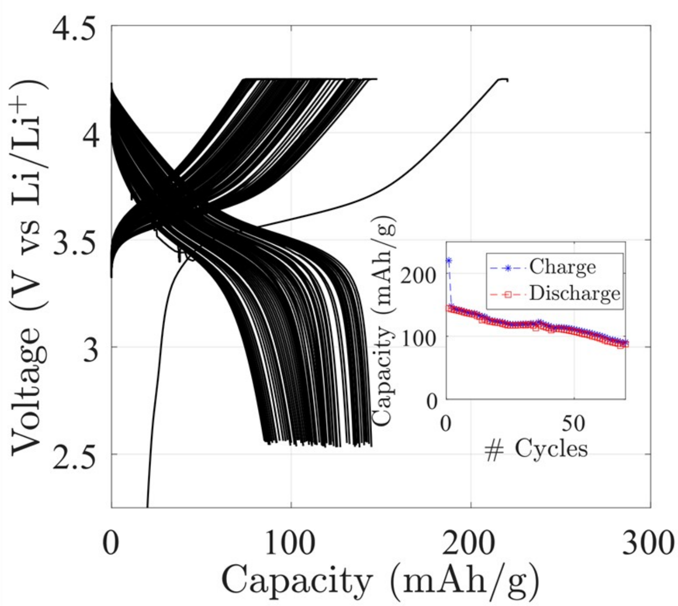

VII. Nyquist impedance plot before charge of cells, with equivalent circuit inserted in the left. Symbols of the equivalent circuit were expressed as follows: R_{SE}, resistance of the bulk SE; R_{ct}, charge-transfer resistance; and W, Warburg impedance.